Regulating Speed in a Neuromuscular Human Running Model

Seungmoon Song and Hartmut Geyer

***Abstract*— A versatile model of human locomotion control can have large impact on the robotics community by eliciting new control ideas for legged robots and providing simulation test-beds for walking assistive robots. There exist neural control models that can generate human-like diverse and robust locomotion behaviors. However, most of the locomotion behaviors have been generated by exploring different sets of low-level control parameters. In this study, we incorporate a higher-layer speed adaptation policy to a previously proposed neuromuscular human model that enables the model to run at speeds ranging from 2.4 to 4.0 ms^{-1} by changing only a single command of the target velocity. In addition, we investigate simple strategies that facilitate speed changes. Among the strategies we explore, modulating the trunk lean shows fast and reliable acceleration and deceleration in average of 0.35 and -0.37 ms^{-2}, respectively.**

I. INTRODUCTION

Human locomotion control models have the potential to elicit new controllers for legged robots and to provide simulation platforms for testing walking assistive devices. The early models of human locomotion control consist of central pattern generators (CPGs) that produce the basic muscle activation rhythms and local reflexes that modulate the muscle activations and the CPGs to adapt to the environment [1]–[3]. Such control structure can generate steady walking and running in a human musculoskeletal simulation [3]. Recently, it is shown that a control model with only reflexes and no CPGs can generate walking close to human kinematics, dynamics and muscle stimulations [4]. More recently, the model is extended to generate robust and diverse 3D human locomotion behaviors [5]. Since the model can generate human-like walking and is robust to external disturbances, it has been adapted to control prosthetic legs [6], [7] and bipedal robots [8]; to test walking assistive devices in simulation [7], [9], [10]; and also to generate graphical characters that walk and run like humans [11].

Changing locomotion speeds and gaits is essential in human locomotion. The reflex-based control model can generate diverse locomotion behaviors and transitions between those behaviors by using different sets of control parameters [5]. For example, the walking speed can be controlled with pre-explored look-up tables of the control parameters [12]. However, it is not compelling that humans store look-up tables of hundreds or thousands of low-level control parameters for all different environments and behaviors; there should be high-level policies that generalize the modulation of the low-level parameters. Some recent studies have proposed that CPGs may play a role in this aspect in human locomotion [13], [14]. For instance, it is shown that by modifying the reflex-based model to control the hip muscles with CPGs and by incorporating a higher-level speed control policy that modulates the lower-level parameters, the walking speed could be successfully controlled by a single command of the target velocity [14].

Here, we investigate how capable the previously proposed neuromuscular controller [5] is in controlling running speeds. Using parameter optimization, we show that the model can generate steady running at different speeds between 2.4∼4.0 ms^{-1} (Sec. III-A). We incorporate a linear speed adaptation policy that allows the model to realize these running speeds with a single command of the target velocity (Sec. III-B). In addition, we investigate simple strategies that facilitate speed changes. Among the strategies we explore, modulating the trunk lean shows best performance (average acceleration and deceleration of 0.35 and -0.37 ms^{-2}, respectively) (Sec. III-C). We also discuss the limitations of the current study which we plan to solve in the future (Sec. IV).

II. NEUROMUSCULAR HUMAN RUNNING MODEL

A. Neuromuscular Human Locomotion Model

We use a sagittal plane neuromuscular human locomotion model adapted from the 3D model proposed in [5] with minimal changes (Fig. 1). The model includes the skeletal segments, the muscle-tendon actuators, and the reflex-based neural controller. The skeletal system consists of 7 rigid segments (trunk, thighs, shanks, and feet) constrained to the sagittal plane, where each leg is actuated by 9 monoarticular and biarticular muscle-tendon units (MTUs). The MTUs exert contraction forces (which are converted to joint torques) based on the muscle dynamics [4] and the stimulation signals ($\mathbf{S}_m$) commanded from the neural controller. The neural controller takes the muscle states ($\mathbf{x}_m$), the global trunk lean angle (θ), the load on the legs ($\mathbf{f}_l$), and the binary foot-ground contact information ($\mathbf{z}_c$) as inputs (which are time-delayed based on the neural transmission delays) and generates muscle stimulation signals. All the properties of the segments, MTUs, and the neural transmission delays are identical to those in [5].

The human model interacts with the ground through contact points located at each ball and heel of the foot. When a contact point engages with the ground, ground reaction forces (GRFs) act on the point. The GRFs are calculated as nonlinear spring-damper forces either in stiction or sliding mode [4].

This work is supported in part by SS: the DARPA M3 program (W91CRB-11-1-0002).

S. Song, and H. Geyer are with the Robotics Institute, Carnegie Mellon University, 5000 Forbes Avenue, Pittsburgh, PA 15213, USA. {smsong,hgeyer}@cs.cmu.edu

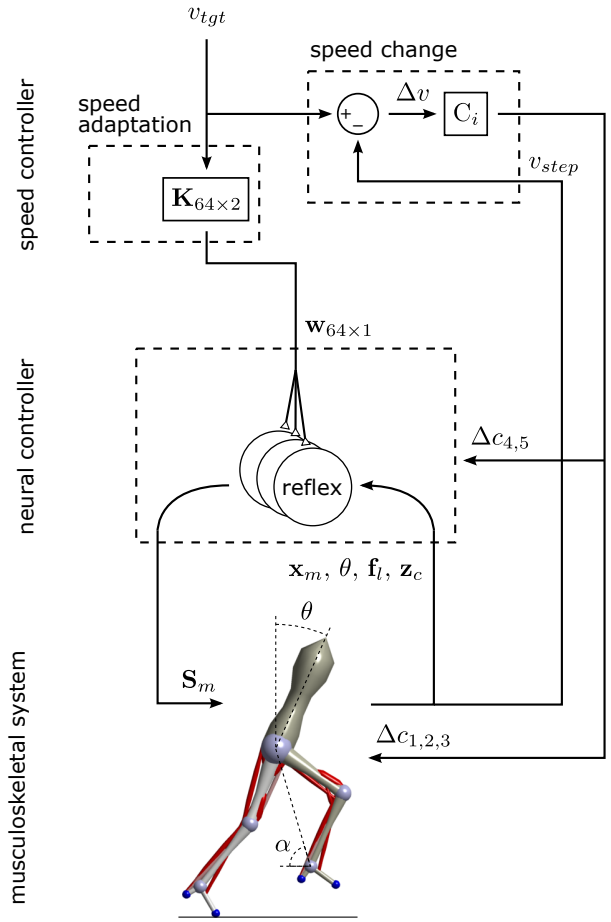

Fig. 1. Speed controller of the neuromuscular human locomotion model. The speed controller modulates the neural controller to control running speeds with a single command of the target velocity.

B. Running Speed Controller

In this paper, we treat the reflex-based neural controller as a black box controller that consists of $n = 64$ control parameters, $\mathbf{w}_{n\times1}$. Given the black box neural controller, we focus on adapting to different running speeds by modulating the control parameters linear to the target running speed and facilitating speed changes with additional speed changing strategies (Fig. 1).

1) Reflex-based neuromuscular running controller: To this end, we first explore the capability of the neuromuscular human locomotion model for running (Sec. III-A). The model does not generate stable running gait in 3D, which is speculated to be caused by the lack of a yaw stabilizing mechanism [5]. If such speculation is correct, the model should be able to generate stable running in the sagittal plan; however, this is not verified. Therefore, we investigate if the sagittal plane model can generate stable running, and explore the range of running speeds by searching different sets of control parameters, $\mathbf{w}$, for different speeds.

2) Speed adaptation policy: Then, we investigate if the model can adapt to different running speeds with a simple policy that modulates the neural control parameters, $\mathbf{w}$, based the target speed (Sec. III-B). We select a policy that sets $\mathbf{w}$ linear to the target running speed, v_{tgt}, as

$$\mathbf{w} = \mathbf{K} \cdot \begin{bmatrix} 1 \\ v_{tgt} \end{bmatrix}. \quad (1)$$

(Not as in [12], [14], we do not select key parameters from $\mathbf{w}$ that show strong trends for different speeds. Analyzing and interpreting the trend of individual neural control parameters are beyond the scope of this paper.) We search for a speed adaptation policy $\mathbf{K}_{n\times2}$ that works for the range of running speeds explored in Sec. II-B.2. Once $\mathbf{K}_{n\times2}$ is set, the model would be able to generate steady running behaviors at different speeds by simply changing the target velocity v_{tgt}, opposed to changing the entire parameter set $\mathbf{w}$ (which would require a large look-up table). We further investigate if the model can change the running speed with the identified linear policy.

3) Speed changing strategies: Lastly, we propose and investigate potential strategies that facilitate speed changes (Sec. III-C). Specifically, we propose simple strategies that modulate either a joint torque or a control parameter of the neural controller linearly proportional to the difference between the current and the target running speed ($\Delta v = v_{tgt} - v_{step}$, where v_{step} is the average velocity during the previous step). The first strategy (C_1) is modulating the hip torque ($\Delta c_1 = \Delta\tau_h$) during the stance phase, where hip extension torque is expected to accelerate the body forward [15], [16]. The second and third strategies ($C_{2,3}$) modulate the knee and ankle torques ($\Delta c_2 = \Delta\tau_k$ and $\Delta c_3 = \Delta\tau_a$) during the late stance phase ($x_{\text{pelvis}} > x_{\text{stance ankle}}$), when the leg thrust contributes to forward propulsion. The last two strategies ($C_{4,5}$) modulate the foot placement (or the swing leg angle α) and the trunk lean (θ) through the high-level control parameters of the neural controller ($\Delta c_4 = \Delta\alpha_{tgt}$ and $\Delta c_5 = \Delta\theta_{tgt}$; α and θ shown in Fig. 1). The foot placement show high correlation with speed changes in human running [16], and modulating the trunk lean is understood as an effective strategy for controlling walking speed [12], [17].

C. Parameter Optimization

We use optimization to search for parameter values. Specifically in each optimization trial we use the covariance matrix adaptation evolution strategy (CMA-ES) [18] to find the values that define the neural control parameters $\mathbf{w}_{64\times1}$, the speed adaptation linear policy $\mathbf{K}_{64\times2}$, or the modulation intensity for speed change $\Delta c_{1\sim5}$. For optimizing $\mathbf{w}$ and $\mathbf{K}$, we set the population size of 64 and maximum of 400 generations of evolution in CMA-ES that takes about 2 days in a modern desktop. For $\Delta c_{1\sim5}$, we set the population size of 8 and maximum of 400 generations, which takes a few hours.

To formulate the parameter searching process as an optimization problem, we need to evaluate the *cost* of a given parameter set. The cost is evaluated by running a neuromuscular physics simulation (MATLAB Simulink/SimMechanics R2014b, ode15s) with the given parameter set and assessing the resulting running behavior. For example, to find the

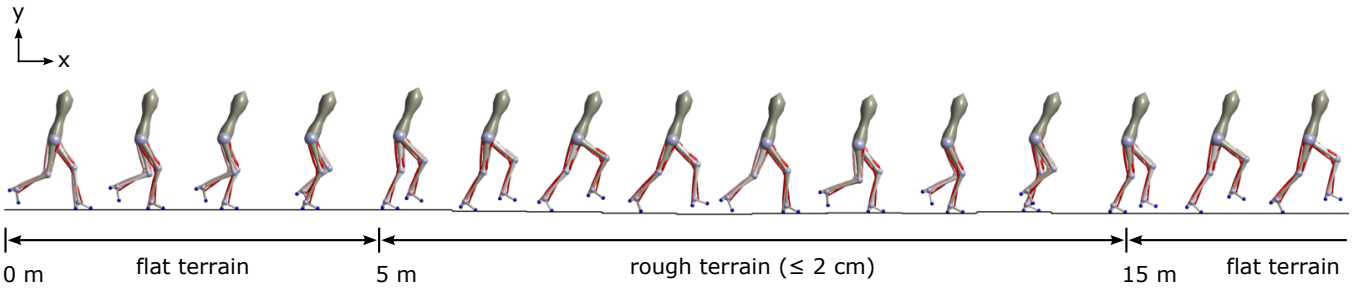

Fig. 2. Neuromuscular physics simulation over rough terrain. The figure shows the snapshots of the human model every 400 ms while running at 3 ms^{-1} across a terrain that includes 10 m of moderate roughness section.

neural control parameters, $\mathbf{w}$, for different running speeds (Sec. III-A), we run a physics simulation to calculate the cost

$$J(\mathbf{w})=\begin{cases} c_1 \left\| v_{avg} - v_{tgt} \right\| + C_E, & \text{if steady run} \quad (2a) \\ c_0 + c_1 t_{DS} + \left\| v_{avg} - v_{tgt} \right\|, & \text{if double stance} \quad (2b) \\ 2c_0 + d_{steady}, & \text{if non-steady} \quad (2c) \\ 3c_0 - x_{fall}, & \text{if fall,} \quad (2d) \end{cases}$$

where x_{fall} is the distance the model runs until falling, d_{steady} is the measure of steady locomotion, t_{DS} is the time duration of double support phase, v_{avg} is the average velocity during steady running, C_E is the metabolic cost of transport, and $c_1 = 100$ is a constant coefficient used to emphasize specific terms. (Details of calculating d_{steady} and C_E are explained in [5].) To impose some robustness on the controller, we run the simulations on a terrain that has a 10 m section of maximum height disturbances of ± 2 cm (Fig. 2). The $c_0 = 10^3$ is large enough to assure Eq. (2a)<(2b)<(2c)<(2d); where Eq. (2d) encourages the model not to fall down, Eq. (2c) induces steady locomotion, and Eq. (2b) searches for running opposed to walking. Once the model successfully produces steady running, CMA-ES searches for energy efficient running at the target speed by minimizing Eq. (2a). (We find that seeding the optimization with a parameter set that allows the model to run 2$\sim$3 steps and including Eq. (2b) in the cost are crucial for searching successful running behaviors.)

III. RESULTS

A. Reflex-Based Neuromuscular Running Controller

We first found successful running at 3.0 ms^{-1} by minimizing the cost Eq. (2) with $v_{tgt} = 3.0$ ms^{-1}. Then we search the range of running speeds the model can generate by changing v_{tgt} by ± 0.1 ms^{-1}. As a result, we found the parameter sets of $\mathbf{w}$ that generate steady running at 2.35$\sim$4.00 ms^{-1} (blue line of Fig. 4-(a)).

The range of running speeds of the model is much less than that of real humans, where normal humans can run in place and sprinters can run at 10 ms^{-1}. The limiting factor for lower speeds is not clear. One possible factor is instability, since it is understood that it is harder to maintain dynamic stability at slower speeds in walking [17]. Although the neural controller includes a reactive foot planner which is supposed to overcome such instability, the current musculoskeletal attachments (which are set considering the range of motion in walking) may not be appropriate for running and prevent the controller from fully using its capability. Inappropriate musculoskeletal attachments may induce MTUs to leave their normal working states (e.g. MTU may overextend or become slack). One evidence that supports this hypothesis of inappropriate attachments is that when the muscles are in use most of them are fully stimulated. (The muscle stimulation timings match that of human running and the full saturation is not due to antagonists fighting each other.) Similar joint torques are generated with much less muscle stimulations in human running, indicating the MTUs of the model are in ineffective states. Inappropriate musculoskeletal attachments may also be limiting faster running, since MTUs cannot produce enough joint torques. Another factor that may be preventing the model from faster running is the simplified upper body. For example, swinging the arms can contribute about 10% in generating vertical propulsion [19]. (With a version of the neural controller and a different musculoskeletal model, [11] have demonstrated running at 3.0$\sim$5.0 ms^{-1}.)

Fig. 3 shows the kinematics and dynamics of the model running at 2.4, 3.2 and 3.9 ms^{-1} along with those data of human running at 3.2 and 4.0 ms^{-1}. The model runs with midfoot strikes (cf. rearfoot strike and forefoot strike). The overall trend of the kinematic and dynamic data agrees with that of human running; the direction of the angles and the joint torques mostly match across the gait cycle, and the vertical GRF has the characteristic single hump. The main differences are observed during the mid swing phase, where the knee angle shows a double hump and the ankle does not extend as much as that of humans. Again, we speculate the inappropriate musculoskeletal attachments as the main factor for these discrepancies. It seems essential to adjust the musculoskeletal model for better prediction of running data, including the muscle activations. For the remaining sections, we focus on the speed control of the model instead of comparing its behaviors with that of humans.

B. Linear Speed Adaptation Policy

Instead of using different sets of the control parameters $\mathbf{w}$, we investigate if the different running speeds can be realized with the linear policy Eq. (1). To find a good policy for

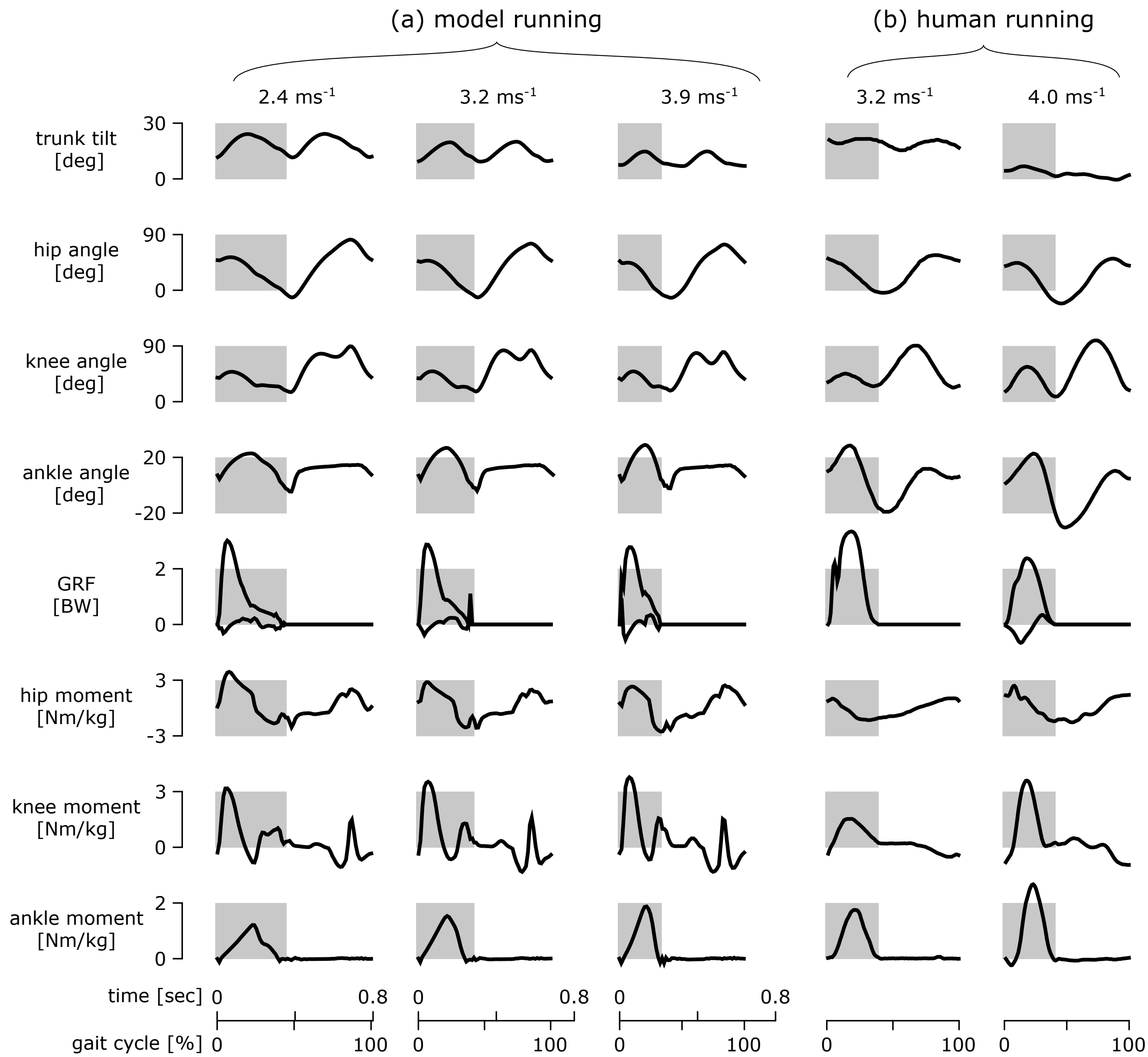

Fig. 3. Running data of the model and humans at different speeds. The kinematic and dynamic data during running are shown in the plot. Positive angles indicate forward trunk (pelvis for humans) lean, hip flexion, knee flexion, and ankle dorsiflexion, where positive joint torques indicate hip extension, knee extension, and ankle plantarflexion. Human running data are those reported in [20] and [21] for 3.2 and 4.0 ms^{-1}, respectively.

adapting to different speeds and making speed changes, we optimize $\mathbf{K}$ that minimizes $J_{acc}(\mathbf{K}) + J_{dec}(\mathbf{K})$, where

$$J_{acc}(\mathbf{K}) = \begin{cases} -c_0 + \Delta t_{acc}, & \text{if speed change} \quad (3a) \\ \left\| v_{avg,1} - v_{tgt,1}^{acc} \right\| + \left\| v_{avg,2} - v_{tgt,2}^{acc} \right\|, & \text{if steady run} \quad (3b) \\ \quad \vdots & \quad \vdots \, . \quad (3c) \end{cases}$$

$J_{dec}(\mathbf{K})$ is the same with v_{tgt1}^{dec}, v_{tgt2}^{dec} and Δt_{dec}. Eq. (3c) represents Eq. (2b$\sim$d), and Eq. (3a) is calculated when the speed change is successfully made (i.e. $\left\| v_{avg,i} - v_{tgt,i}^{acc} \right\| < 0.05$ for both $i = 1, 2$). The target values are set as $v_{tgt,1}^{acc} = v_{tgt,2}^{dec} = 2.4$ ms^{-1} and $v_{tgt,2}^{acc} = v_{tgt,1}^{dec} = 3.9$ ms^{-1}. We run two simulations to calculate each $J_{acc}(\mathbf{K})$ and $J_{dec}(\mathbf{K})$.

By minimizing the cost Eq. (3) we obtain a linear speed adaptation policy $\mathbf{K}$ that allows the model to run at different speeds between 2.4$\sim$3.9 ms^{-1} (black line of Fig. 4-(a)). Interestingly, the relationship between the commanded velocity, v_{tgt}, and the actual running speed shows a S-shape, indicating that including a nonlinear mapping such as $\mathbf{w} = \mathbf{K} \cdot \begin{bmatrix} 1 \\ f(v_{tgt}) \end{bmatrix}$ will produce better speed adaptation. Fig. 4-(b) shows the step lengths of running at different speeds. (The step lengths of human running are plotted for comparison.) Since CMA-ES does not guarantee global optimum (as other nonlinear optimizers), some of the optimization solutions are different types of local minima, generating inconsistent step length–velocity relationship (blue line). On the other hand,

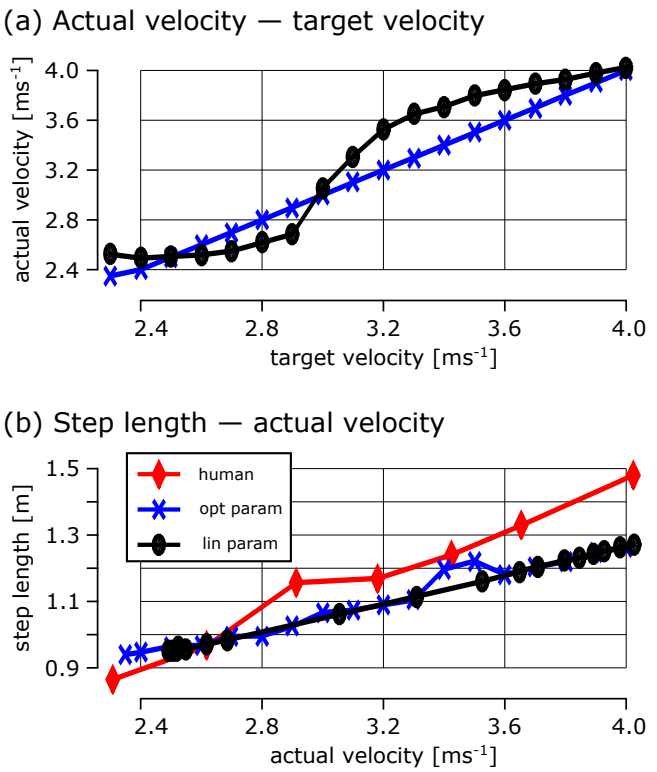

Fig. 4. Relationships between the target velocities, the actual velocities and the step lengths. Step lengths of human running across different running speeds are from [22].

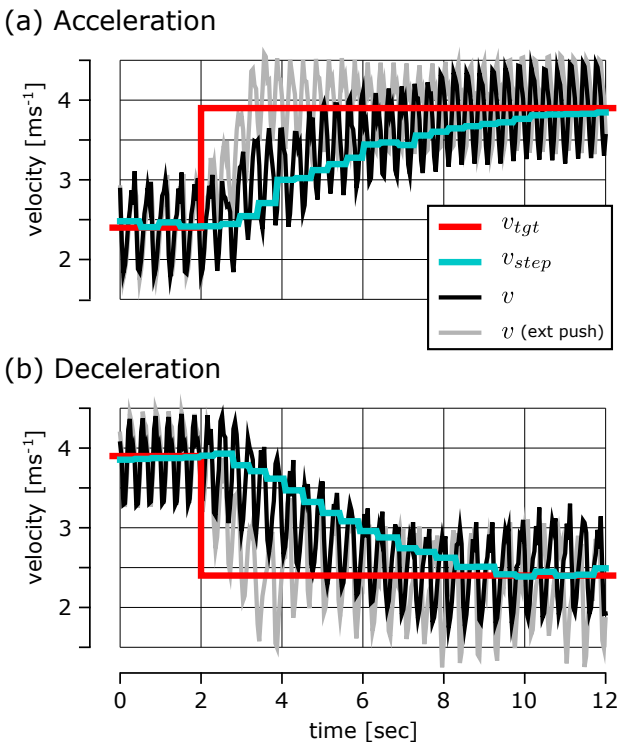

Fig. 5. Acceleration and deceleration induced by the linear speed adaptation policy. Speed changes facilitated by external pushes (ext push) are also plotted.

the running behaviors generated by the linear speed adaptation policy $\mathbf{K}$ have consistent properties across different speeds. This reveals an advantage of using a unified policy of generating different behaviors comparing to using a look-up table of different sets of parameters found by independent optimization trials.

The linear speed adaptation policy can also be used for inducing speed changes (Fig. 5). The speed changes between 2.4 and 3.9 ms^{-1} are realized by changing the target velocity, v_{tgt}, instantly from one to the other (red lines). The average acceleration and deceleration are 0.18 and -0.26 ms^{-2}, respectively (Table I), which are much slower comparing to humans. However, we find that the linear speed adaptation policy can adapt to faster speed changes induced by a separate speed changing strategy. For instance, when faster speed changes happen by external pushes on the trunk, the model makes faster acceleration and deceleration (gray lines). Such observation motivated us to investigate explicit speed changing strategies that run independently with the speed adaptation policy.

C. Speed Changing Strategies

In this section, we investigate the speed changing strategies explained in Sec. II-B.3. We optimize the intensities of each strategy Δc_i $(i = 1, 2, \cdots, 5)$ separately for acceleration and deceleration by minimizing $J_{acc}(\Delta c_i)$ and $J_{dec}(\Delta c_i)$ of Eq. (3), respectively. (Note that the speed adaptation policy, $\mathbf{K}$, is not changed from that identified in Sec. III-B.) The results are shown in Table I. The Δc_i values should be larger than zero to be in line with the functional purpose of each speed changing strategy. For example, we expected $\Delta c_1 = \Delta\tau_h > 0$ (Nm)/(ms^{-1}) to facilitate speed changes, since it adds hip extension torque during stance for acceleration and reduces it for deceleration. However, the optimized $\Delta c_1 = \Delta\tau_h$ and $\Delta c_4 = \Delta\alpha_{tgt}$ have negative values. We speculate that positive $\Delta\tau_h$ modulates the trunk lean angle in the direction that hinders speed changes. For $\Delta c_4 = \Delta\alpha_{tgt}$, the optimization found a special case where the model makes an abrupt deceleration by first increasing the running speed. Deceleration made by $\Delta c_2 = \Delta\tau_k$ also is a similar case; the model first accelerates by increasing the leg propulsion and then loses stability of the stance leg (i.e. instantaneous large

TABLE I
SPEED CHANGES WITH DIFFERENT STRATEGIES

		no ctrl	ext push	$\Delta\tau_h$	$\Delta\tau_k$	$\Delta\tau_a$	$\Delta\alpha_{tgt}$	$\Delta\theta_{tgt}$
accel	Δc_i ($\cdot$ /ms^{-1})	-	-	-18 Nm	8 Nm	10 Nm	3 deg	28 deg
	2.4 $\rightarrow$ 3.9 (ms^{-2})	0.18	0.96	0.25	0.19	0.23	0.27	0.35
decel	Δc_i ($\cdot$ /ms^{-1})	-	-	-7 Nm	5 Nm	8 Nm	-3 deg	21 deg
	3.9 $\rightarrow$ 2.4 (ms^{-2})	-0.26	-0.86	-0.33	(-0.52)	-0.31	(-0.43)	-0.37

(accel: acceleration, decel: deceleration, ctrl: control, ext: external, positive joint torques indicate extension torques)

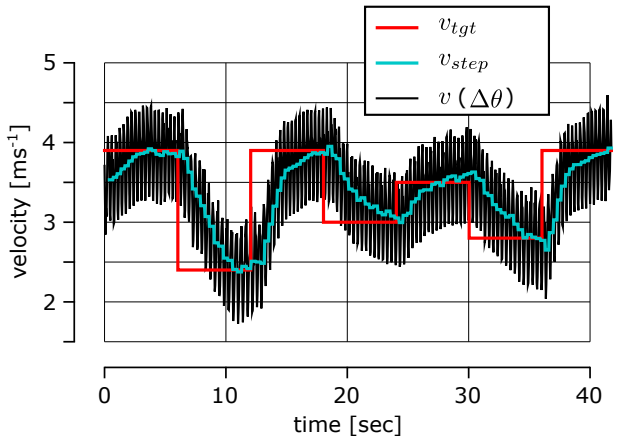

Fig. 6. Speed control of the neuromuscular human running model. The plot shows that the model can track target velocities arbitrarily changing every 6 second. The model used the speed changing strategy of modulating the trunk lean for both acceleration and deceleration.

knee flexion during stance) that causes abrupt deceleration. These strategies are specialized for the given scenario and are difficult to be generalized for different speed changes. (Constraints that prevents these special scenarios should be added in the optimization routine to obtain reliable strategies.) Other strategies ($\Delta c_{1,3,5}$) show consistent speed changes. Among them, the trunk lean modulation strategy ($\Delta c_5 = \Delta\theta_{tgt}$) makes the largest acceleration and deceleration of 0.35 and -0.37 ms^{-1}, respectively. This strategy generalizes for different target velocity profiles (Fig. 6).

IV. SUMMARY AND FUTURE DIRECTIONS

Better control models of human locomotion can impact the field of robotics. In this contribution, we investigated the capability of a previously proposed neuromuscular human locomotion model [5] in controlling running speeds. With different sets of control parameters, the sagittal plane version of the model were able to generate steady running at different speeds from 2.4 to 4.0 ms^{-1}. Such steady running behaviors could also be generated by changing only the target velocity with a linear speed adaptation policy. Changing the target velocity of the speed adaptation policy also induced speed changes, although the changes are relatively slow (average acceleration and deceleration of 0.18 and -0.26 ms^{-2}, respectively). We investigated simple strategies that can expedite these speed changes. Among the strategies we explored, modulating the trunk lean showed the best performance (average acceleration and deceleration of 0.35 and -0.37 ms^{-2}, respectively) among the reliable ones.

The proposed speed controller is not complete in many aspects. First, the original neuromuscular model should be updated to better predict the human running behaviors. This includes revising the musculoskeletal properties and may also involve introducing more functional control modules specific for running. Second, the linear speed control policy can be further polished. For instance, we can analyze the neural control parameters and select the parameters essential for speed control as in the previous study [12]. Lastly, the speed changing strategies we proposed are immature. For example, some strategies directly modulate joint torques instead of doing so through the muscle actuators. In addition, we have not investigated the effect of combining the strategies, which may enhance the speed changing performance by much. We plan to solve these limitations which would lead us to a better human locomotion control model.

REFERENCES

[1] G. Taga, "A model of the neuro-musculo-skeletal system for human locomotion," *Biological cybernetics*, vol. 73, no. 2, pp. 97–111, 1995.

[2] N. Ogihara and N. Yamazaki, "Generation of human bipedal locomotion by a bio-mimetic neuro-musculo-skeletal model," *Biological cybernetics*, vol. 84, no. 1, pp. 1–11, 2001.

[3] K. Hase, K. Miyashita, S. Ok, and Y. Arakawa, "Human gait simulation with a neuromusculoskeletal model and evolutionary computation," *The Journal of Visualization and Computer Animation*, vol. 14, no. 2, pp. 73–92, 2003.

[4] H. Geyer and H. Herr, "A muscle-reflex model that encodes principles of legged mechanics produces human walking dynamics and muscle activities," *Neural Systems and Rehabilitation Engineering, IEEE Transactions on*, vol. 18, no. 3, pp. 263–273, 2010.

[5] S. Song and H. Geyer, "A neural circuitry that emphasizes spinal feedback generates diverse behaviours of human locomotion," *The Journal of physiology*, 2015.

[6] M. F. Eilenberg, H. Geyer, and H. Herr, "Control of a powered ankle–foot prosthesis based on a neuromuscular model," *Neural Systems and Rehabilitation Engineering, IEEE Transactions on*, vol. 18, no. 2, pp. 164–173, 2010.

[7] N. Thatte and H. Geyer, "Towards local reflexive control of a powered transfemoral prosthesis for robust amputee push and trip recovery," in *Intelligent Robots and Systems (IROS 2014), 2014 IEEE/RSJ International Conference on*. IEEE, 2014, pp. 2069–2074.

[8] Z. Batts, S. Song, and H. Geyer, "Toward a virtual neuromuscular control for robust walking in bipedal robots," in *Intelligent Robots and Systems (IROS 2015), 2015 IEEE/RSJ International Conference on*. IEEE, accepted.

[9] W. van Dijk and H. van der Kooij, "Optimization of human walking for exoskeletal support," in *Rehabilitation Robotics (ICORR), 2013 IEEE International Conference on*. IEEE, 2013, pp. 1–6.

[10] K. Seo, S. Hyung, B. K. Choi, Y. Lee, and Y. Shim, "A new adaptive frequency oscillator for gait assistance," in *Robotics and Automation (ICRA), 2015 IEEE International Conference on*. IEEE, 2015, pp. 5565–5571.

[11] J. M. Wang, S. R. Hamner, S. L. Delp, and V. Koltun, "Optimizing locomotion controllers using biologically-based actuators and objectives." *ACM Trans. Graph.*, vol. 31, no. 4, p. 25, 2012.

[12] S. Song and H. Geyer, "Regulating speed and generating large speed transitions in a neuromuscular human walking model," in *Robotics and Automation (ICRA), 2012 IEEE International Conference on*. IEEE, 2012, pp. 511–516.

[13] F. Dzeladini, J. Van Den Kieboom, and A. Ijspeert, "The contribution of a central pattern generator in a reflex-based neuromuscular model," *Frontiers in human neuroscience*, vol. 8, 2014.

[14] N. Van der Noot, A. Ijspeert, and R. Ronsse, "Biped gait controller for large speed variations, combining reflexes and a central pattern generator in a neuromuscular model," in *Robotics and Automation (ICRA), 2015 IEEE International Conference on*. IEEE, 2015, pp. 6267–6274.

[15] M. H. Raibert, *Legged robots that balance*. MIT press, 1986.

[16] M. Qiao and D. L. Jindrich, "Task-level strategies for human sagittal-plane running maneuvers are consistent with robotic control policies," *PLoS One*, vol. 7, no. 12, p. e51888, 2012.

[17] D. G. Hobbelen and M. Wisse, "Controlling the walking speed in limit cycle walking," *The International Journal of Robotics Research*, vol. 27, no. 9, pp. 989–1005, 2008.

[18] N. Hansen, "The cma evolution strategy: a comparing review," in *Towards a new evolutionary computation*. Springer, 2006, pp. 75–102.

[19] R. N. Hinrichs, P. R. Cavanagh, and K. R. Williams, "Upper extremity function in running. i: Center of mass and propulsion considerations," *JAB*, vol. 3, no. 3, 2010.

[20] T. F. Novacheck, "The biomechanics of running," *Gait & posture*, vol. 7, no. 1, pp. 77–95, 1998.
[21] S. R. Hamner, A. Seth, and S. L. Delp, "Muscle contributions to propulsion and support during running," *Journal of biomechanics*, vol. 43, no. 14, pp. 2709–2716, 2010.
[22] G. Cavagna, P. Franzetti, N. Heglund, and P. Willems, "The determinants of the step frequency in running, trotting and hopping in man and other vertebrates." *The Journal of Physiology*, vol. 399, no. 1, pp. 81–92, 1988.